

Update on SPI experiments at JET-ILW in 2019-2020\*

**S.N. Gerasimov**<sup>1</sup> on behalf of L.R. Baylor<sup>2</sup>, A. Boboc<sup>1</sup>, I.S. Carvalho<sup>3</sup>, P. Carvalho<sup>1</sup>, I.H. Coffey<sup>1,4</sup>, D. Craven<sup>1</sup>, J. Flanagan<sup>1</sup>, A. Huber<sup>5</sup>, V. Huber<sup>6</sup>, S. Jachmich<sup>7</sup>, I. Jecu<sup>1</sup>, E. Joffrin<sup>8</sup>, D. Kos<sup>1</sup>, S.I. Krasheninnikov<sup>9</sup>, U. Kruezi<sup>6</sup>, M. Lehnen<sup>6</sup>, P.J. Lomas<sup>1</sup>, A. Manzanares<sup>10</sup>, M. Maslov<sup>1</sup>, A. Peacock<sup>1</sup>, P. Puglia<sup>1</sup>, S. Silburn<sup>1</sup>, F.G. Rimini<sup>1</sup>, R.D. Smirnov<sup>9</sup>, C. Stuart<sup>1</sup>, H. Sun<sup>1</sup>, D. Shiraki<sup>3</sup>, J. Wilson<sup>1</sup>, L.E. Zakharov<sup>14,15</sup> and JET Contributors<sup>16</sup>  
EUROfusion Consortium, JET, Culham Science Centre, Abingdon, OX14 3DB, UK

<sup>1</sup> UKAEA/CCFE, Culham Science Centre, Abingdon, OX14 3DB, UK  
<sup>2</sup> Oak Ridge National Laboratory, Oak Ridge, TN 37831, USA  
<sup>3</sup> IPFN, Instituto Superior Técnico, Universidade de Lisboa, Lisboa, Portugal  
<sup>4</sup> Astrophysics Research Centre, Queen's University, Belfast, BT7 1NN, UK  
<sup>5</sup> Forschungszentrum Jülich GmbH, Institut für Energie- und Klimaforschung-Plasmaphysik, Partner of TEC, 52425 Jülich, Germany  
<sup>6</sup> Jülich Supercomputing Centre, Forschungszentrum Jülich, 52425 Jülich, Germany  
<sup>7</sup> ITER Organization, Route de Vinon, CS 90 046, 13067 Saint Paul Lez Durance, France  
<sup>8</sup> CEA, IRFM, F-13108 Saint-Paul-lez-Durance, France  
<sup>9</sup> Laboratorio Nacional de Fusión, CIEMAT, 28040 Madrid, Spain  
<sup>10</sup> Department of Physics, University of Helsinki, P.O. Box 43, FIN - 00014, Finland  
<sup>11</sup> LiW Fusion P.O. Box 2391, Princeton NJ 08543, USA  
<sup>12</sup> See 'Overview of JET results for optimizing ITER operation' J. Mailloux et al 2022 (https://doi.org/10.1088/1741-4326/ac47b4) for the JET Contributors

\* This poster is an excerpt from the "Mitigation of disruption electro-magnetic load with SPI on JET-ILW" manuscript due to be submitted to the NF by August this year

**Disruptions are an inherent property of tokamak plasmas, which cannot be completely eliminated.** The consequences of disruptions are especially dangerous for large machines like JET and even more so for ITER. Disruptions can cause large Electro-Magnetic (EM) loads on the tokamak components and huge thermal loads on the Plasma Facing Components (PFCs). Moreover, high-energy powerful Runaway Electron (RE) beams may arise during disruptions and cause serious damage of the machine.

**1. JET SPI** The SPI can fire pellets with a diameter of  $d = [4.57, 8.1, 12.5]$  mm and pellet compositions of D2, Ne with D2 shell, Ne+D2 mixture, Ar and Ar + D2 sandwich pellets. The pellets are released by means of propellant gas or a mechanical punch.

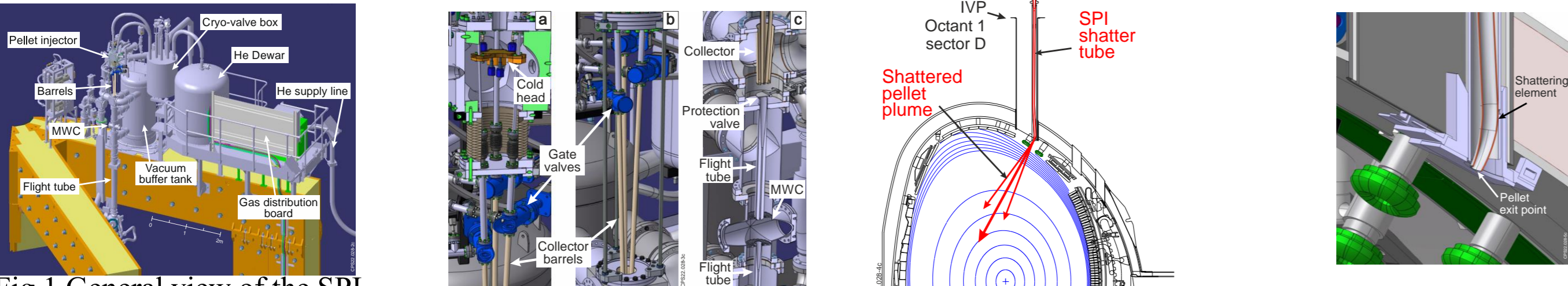


Fig.1 General view of the SPI installation in Octant 1

Fig.2 The sequence of the pellet route from (a) Cold head of the injector, then (b) through Gate valves and Collector barrels to (c) Collector and Flight tube with Protection valve to the Microwave Cavity (MWC) and next Flight tube to the vacuum vessel.

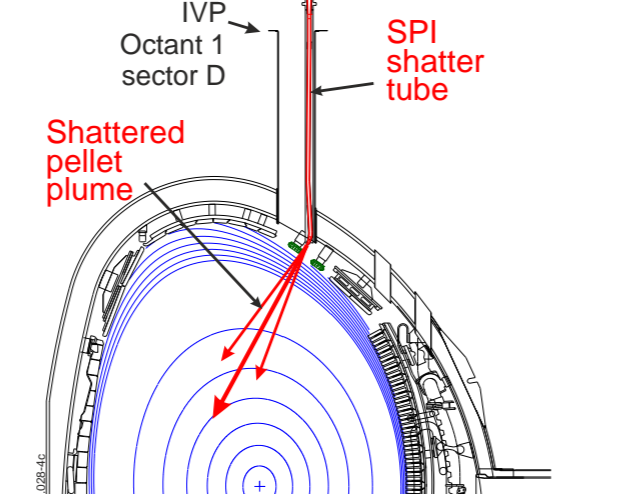
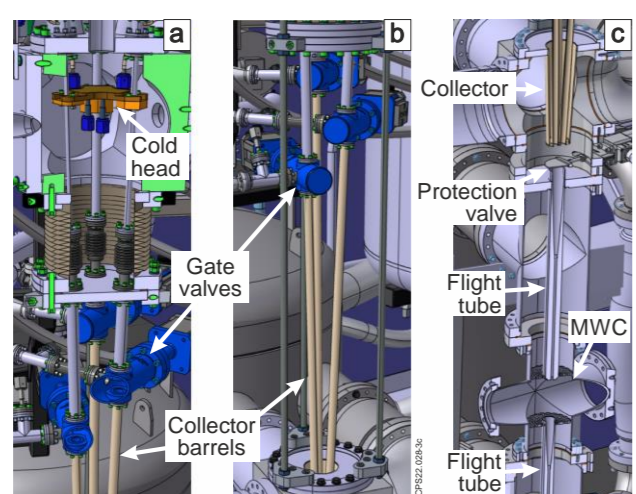


Fig.3 SPI shatter tube (in red) fitted in guiding tube in the Intermediate Vertical Port (IVP) in Octant 1 sector D.

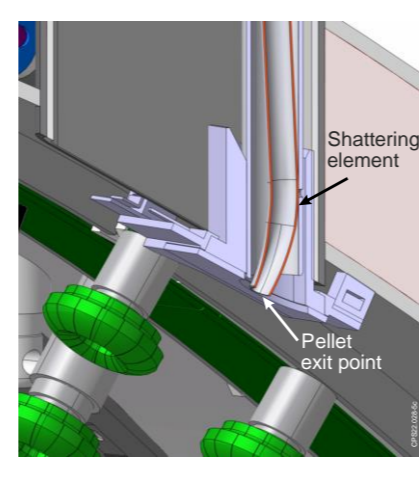


Fig.4 The entry point of the pellet into the JET vacuum vessel. The shatter tube with the shattering element is in red.

**2. DIAGNOSTICS**

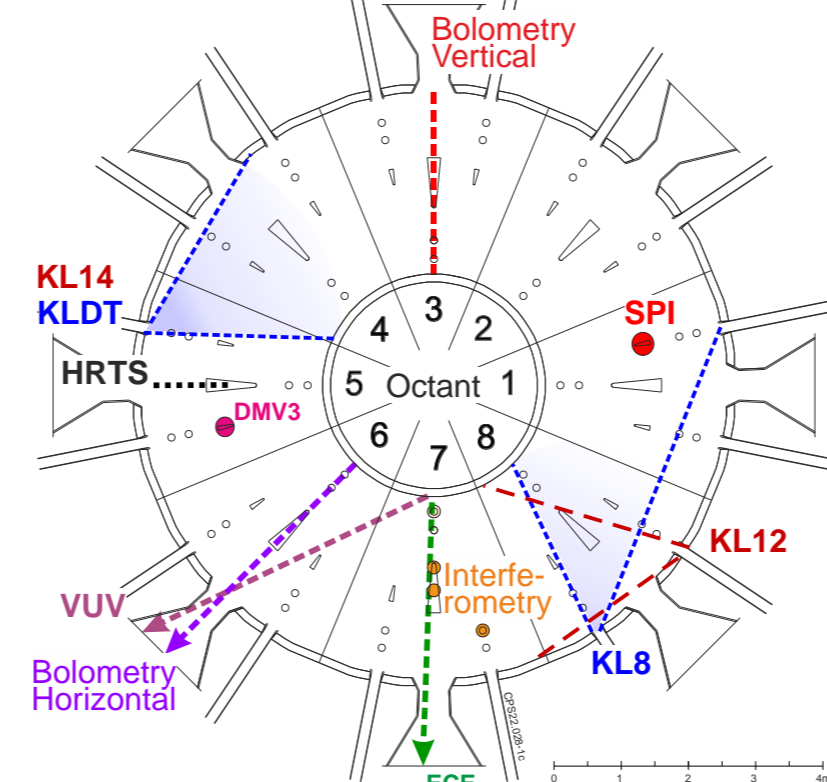


Fig.5 JET vessel plan view: SPI, Fast Visible (KL8 and KLDT) and Infrared (KL12 and KL14) camera views, Bolometry, Interferometry, ECE, VUV, HRTS and DMV3

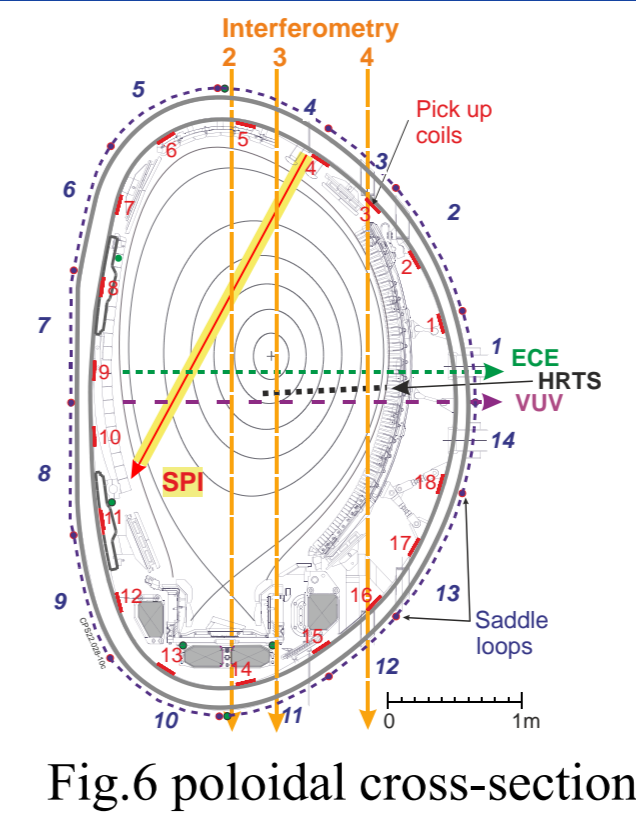


Fig.6 poloidal cross-section.

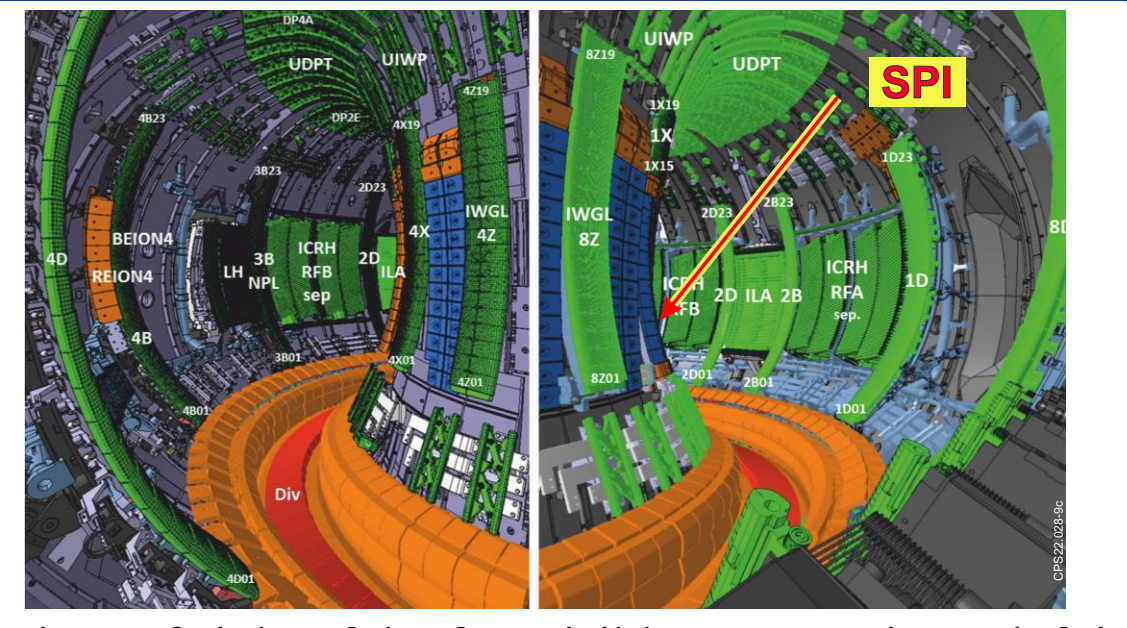
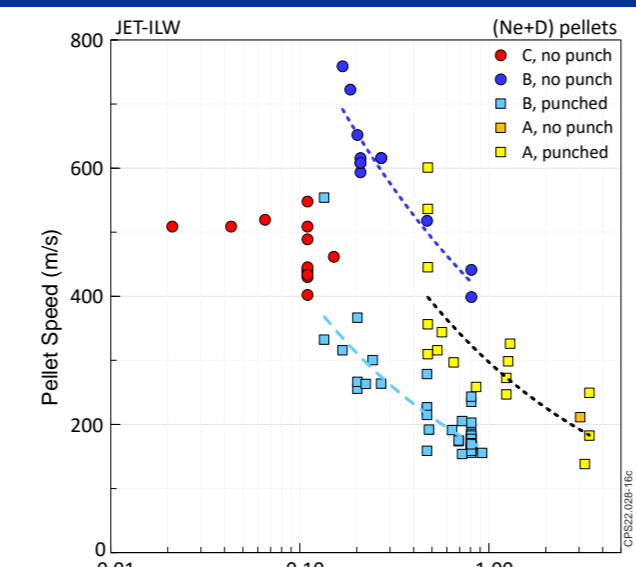


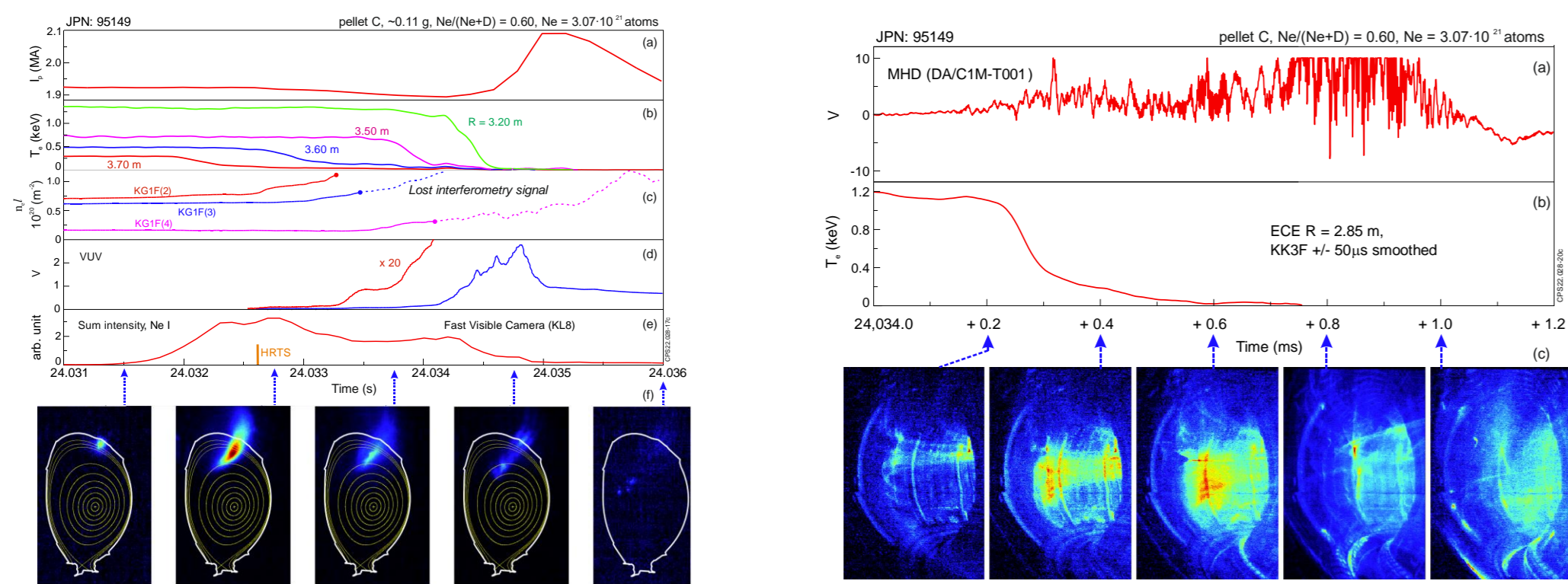
Fig.7 Lines of sight of the fast visible camera views: left is KLDT camera view from Oct.5 to Oct.4 and Oct.3; right is KL8 camera view from close to the midplane in Oct 8 towards

Fig.10 The speed of a pellet depends on the mass of the pellet, the diameter of the barrel, and whether a mechanical punch is used. However, comparison between barrels can be very misleading. The larger barrel has less restriction for the propellant gas. Thus, a medium size pellet B is faster than a small size pellet C with the same mass



**4.1 CHARACTERIZATION OF DISRUPTIONS INSTIGATED BY PELLETS**

The SPI system on JET is intended to be used to study the physics of disruption instigated by pellets and is not used as a true disruption mitigation system. The experiment was performed with  $I_p = (1.1 - 3.1)$  MA, internal (thermal + poloidal magnetic) pre-disruptive plasma energy  $W_{tot}^{dis} = W_p^{dis} + W_{mag}^{dis} = (1 - 15)$  MJ mainly with Ne + D2 pellet composition, but also with Ar pellets.



Ne I (1.8 eV) is not visible during CQ!

Fig.11 Small pellet C instigated disruption: (a) plasma current, (b) electron temperature, (c) line density, (d) light, (e) Ne I intensity, (f) Fast visible camera KL8, 50 μs frames, Ne I filter, the equilibrium shown for illustration purpose only.

Ohmic plasma  $I_p = 2$  MA

**4.2 CHARACTERIZATION OF DISRUPTIONS INSTIGATED BY PELLETS**

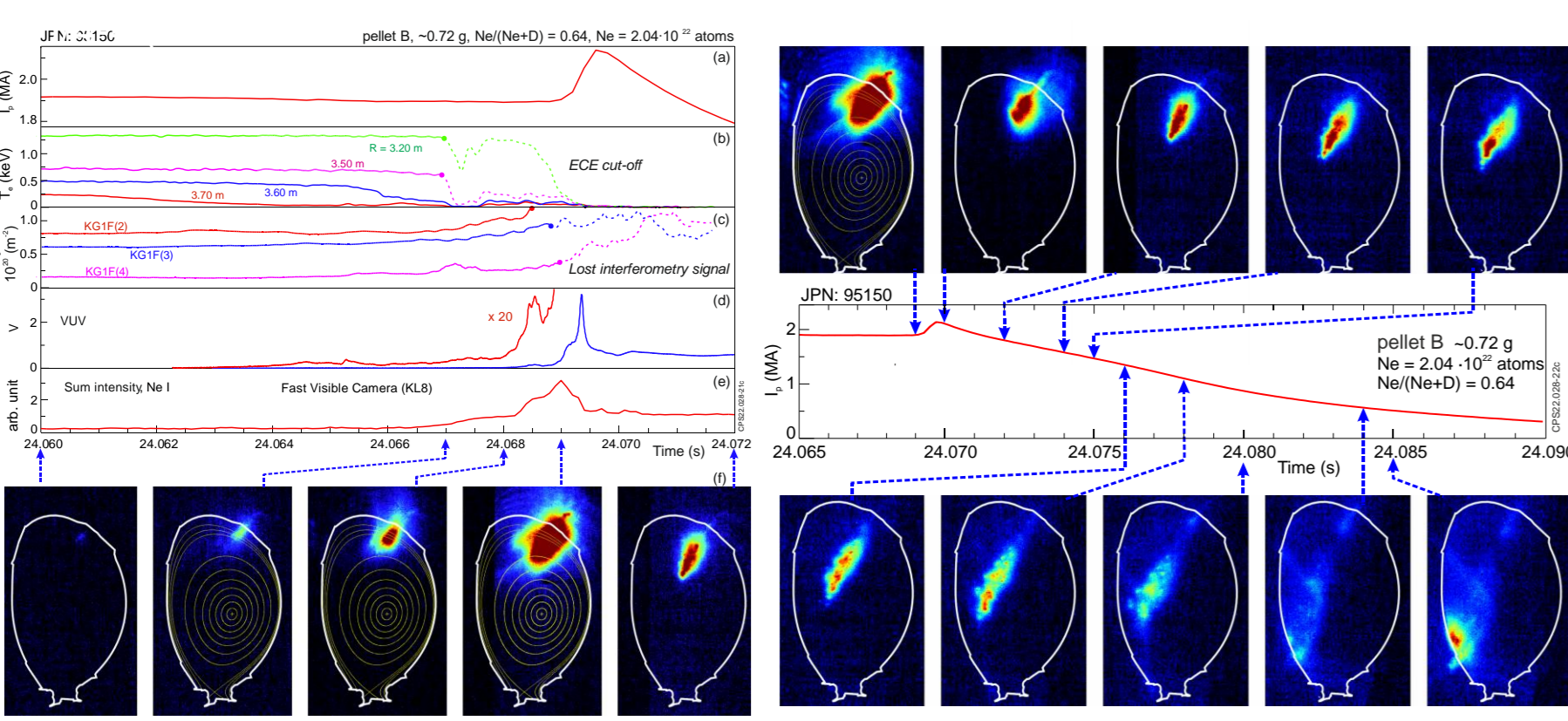


Fig.12 Medium pellet B instigated disruption. pellet fragments (Ne I line), are clearly visible throughout CQ even at the end of CQ when the pellet fragments hit the inter wall.

Ohmic plasma  $I_p = 2$  MA

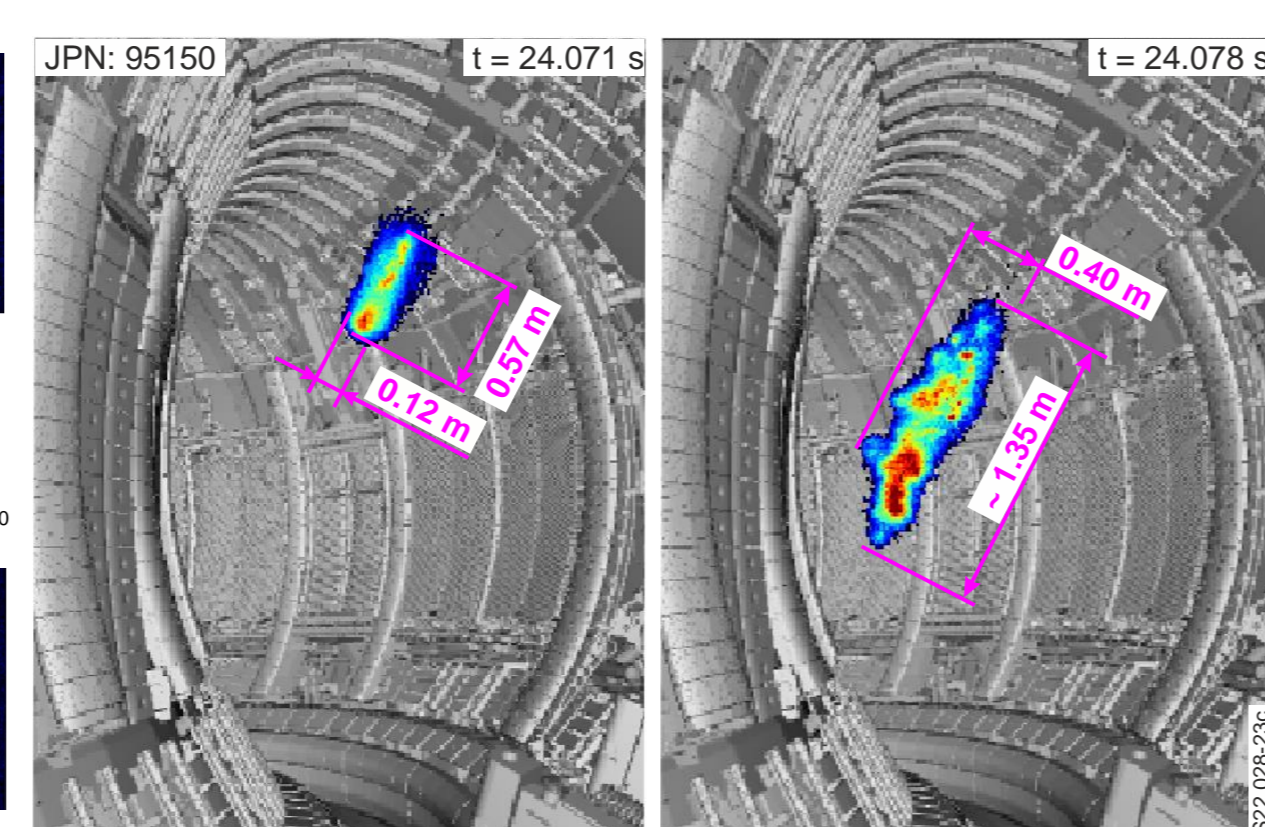


Fig.13 Fragment flies with non-uniform speed with a large spread of in range (66 - 177) m/s. The cloud of neutral Ne lengthens and widens with time.

**5 EFFICACY OF SMALL & MEDIUM PELLETS**

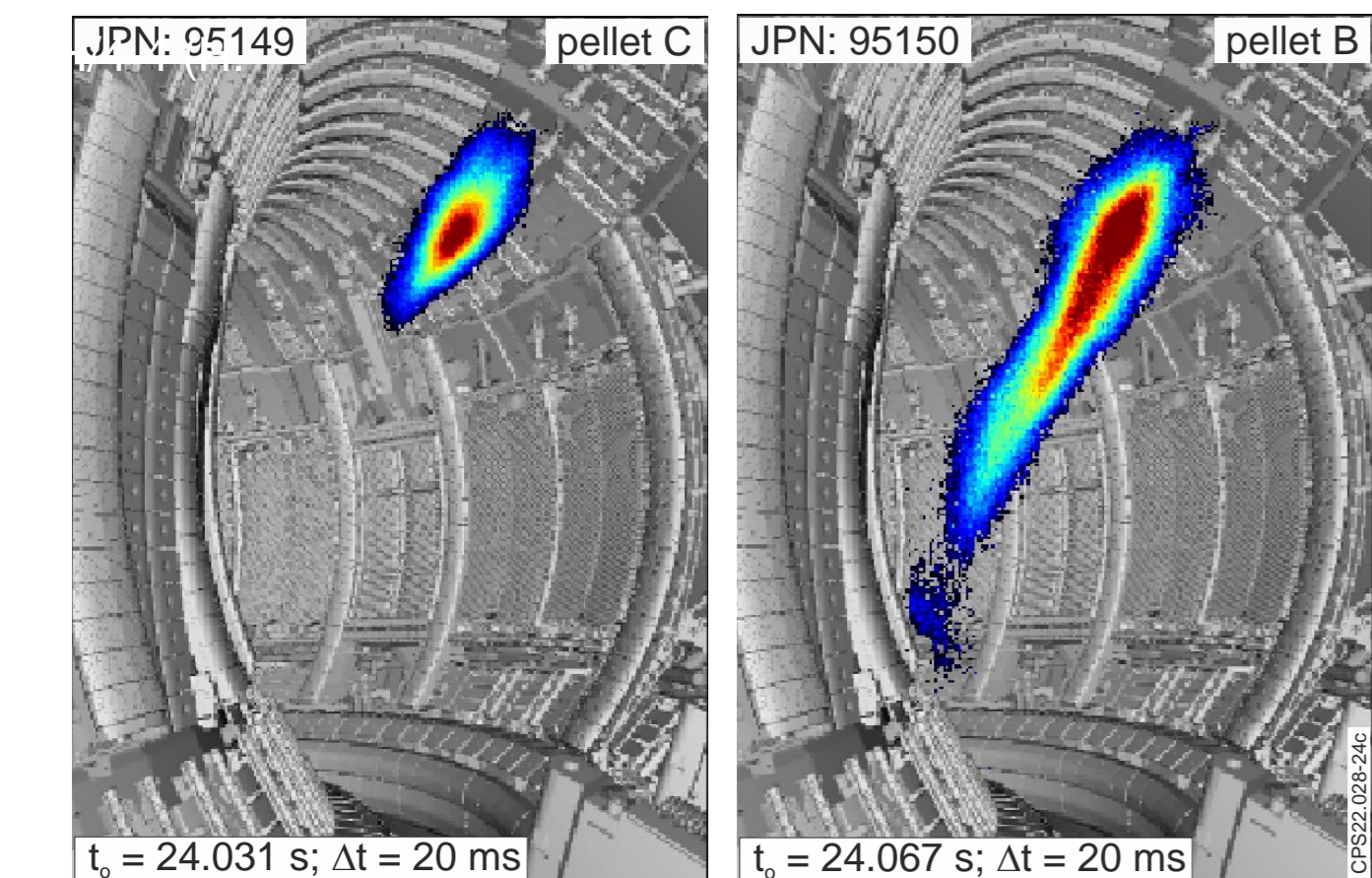


Fig.14 Sum of all Ne I images starting from cooling and further in the process of the CQ for small pellet C and medium pellet B. Moving through the plasma, the cloud of neutral Ne lengthens, but does not expand in a cone, remaining in the form of the cylinder,

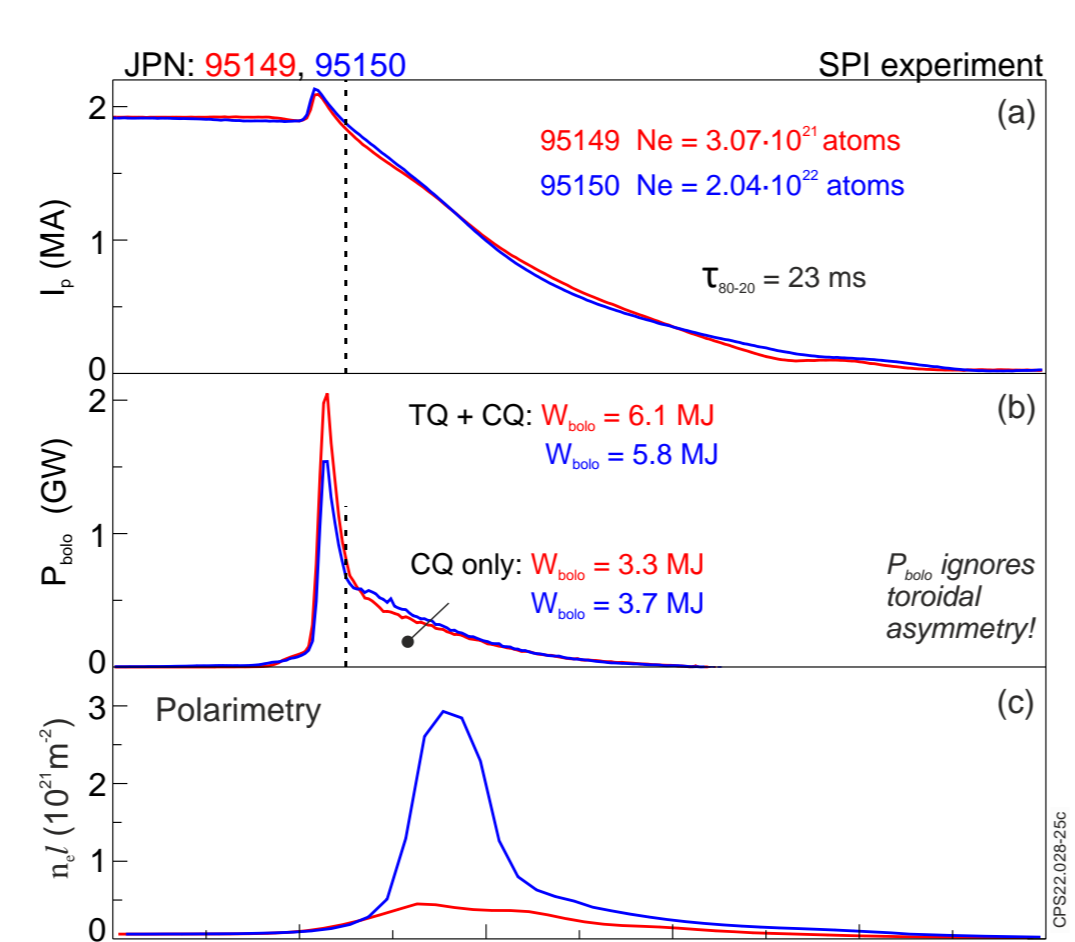


Fig.15 Despite the large difference in the parameters of pellets C and B, the number of Ne and D atoms and the speed of the pellets, their efficiency, in terms of  $\tau_{80-20}$  and measured radiated energy during SPI initiated disruption is approximately the same

Ohmic plasma  $I_p = 2$  MA

**6 EFFECT OF THE PELLETS ON CQ DURATION**

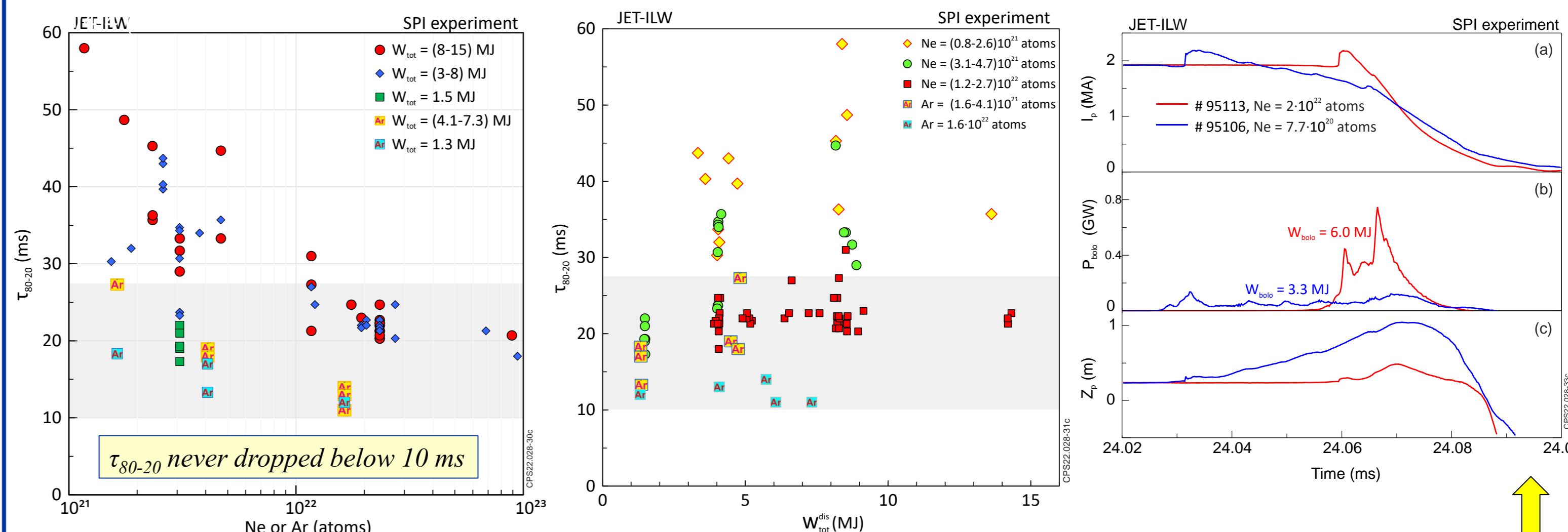


Fig.16 Pellet with a high content of Ne or Ar can reduce the CQ duration to below the upper required JET threshold  $\tau_{80-20} < 27.5$ ms.

Fig.17 Plasmas with high internal (thermal + poloidal magnetic) energy require a high content of Ne or Ar pellet to obtain a short CQ duration, Ar pellets are more efficient than Ne pellets..

Fig.18 Pellets with a very small amount of Ne

**Pellets with a very small amount of Ne, and accordingly large amount of D, instead of causing a mitigated CQ, create the conditions for a "cold" VDE, which is the worst-case scenario for plasma termination.**

**7 VDE/AVDE AND SPI**

**AVDEs are dangerous for two reasons: firstly, the plasma surface currents that the plasma shared with the "wall" can melt beryllium PFCs, and secondly, AVDEs can create large sideways forces acting on the vessel. Both destructive impacts were regularly observed on JET-ILW.**

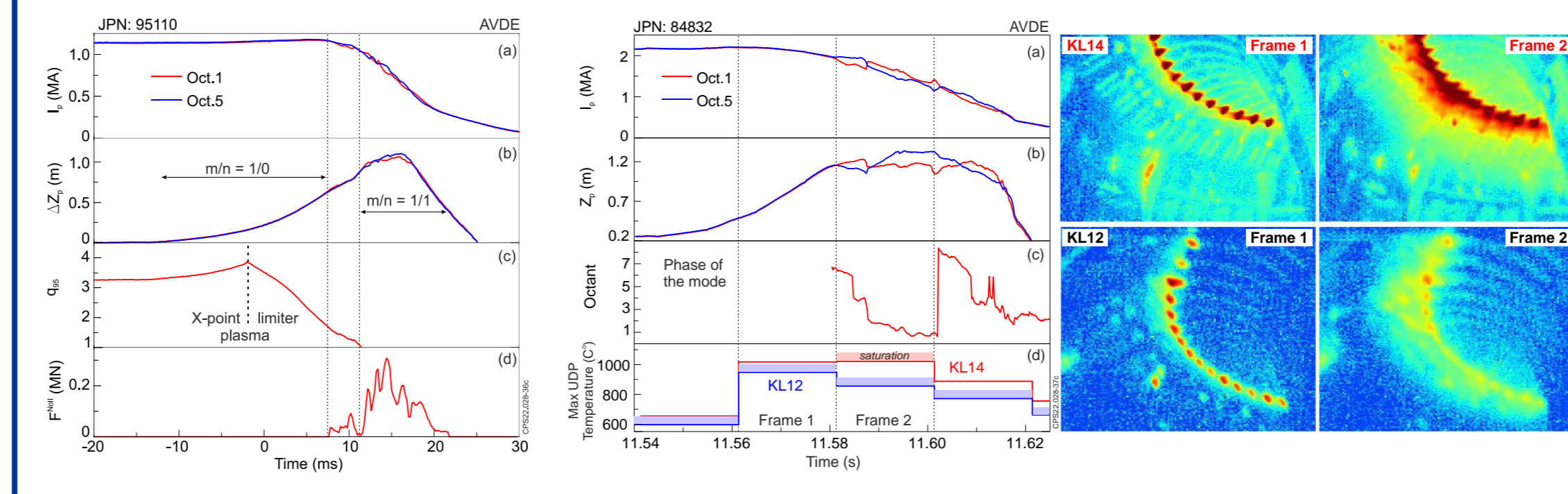


Fig.19 Two phases of VDE: axisymmetric ( $m/n = 1/0$ ) and asymmetric ( $m/n = 1/1$ ).

Fig.20 AVDE heating of beryllium plate, left. maximum temperature of the plate recorded by KL14 and KL12 infrared cameras, Be temperature range: (500 - 1000)° C.

Fig.21 EFIT reconstruction in the end of axisymmetric phase of VDE. The inserted image is low field site of the melted Be taken during inspection.

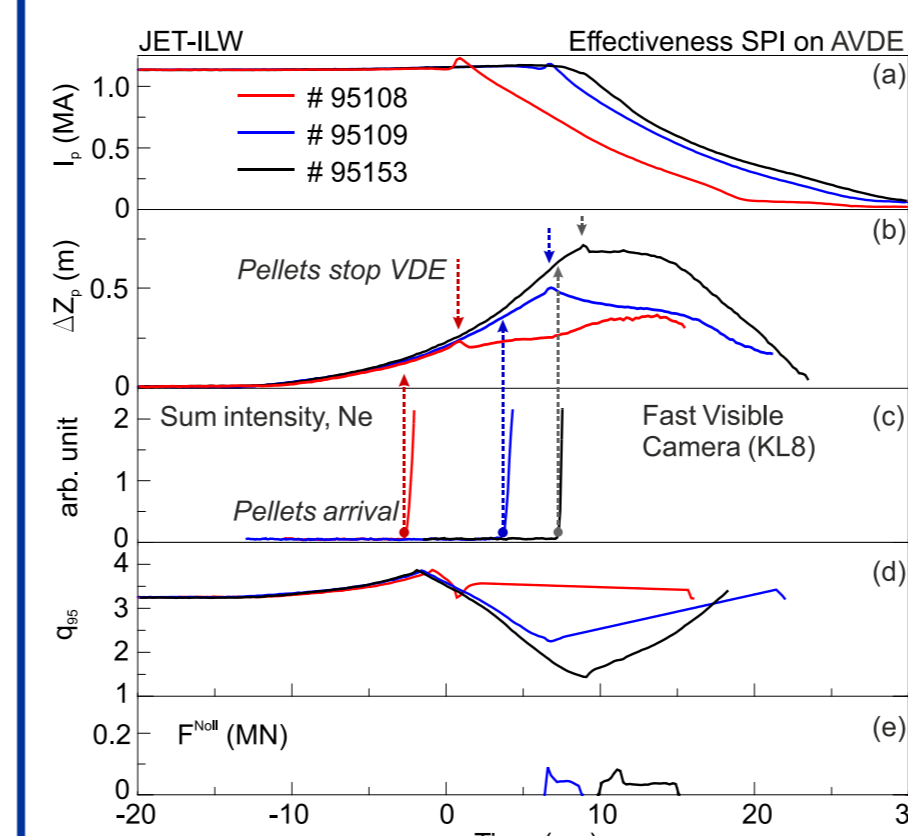


Fig.22 Pellets arrival stopping vertical movement of plasma

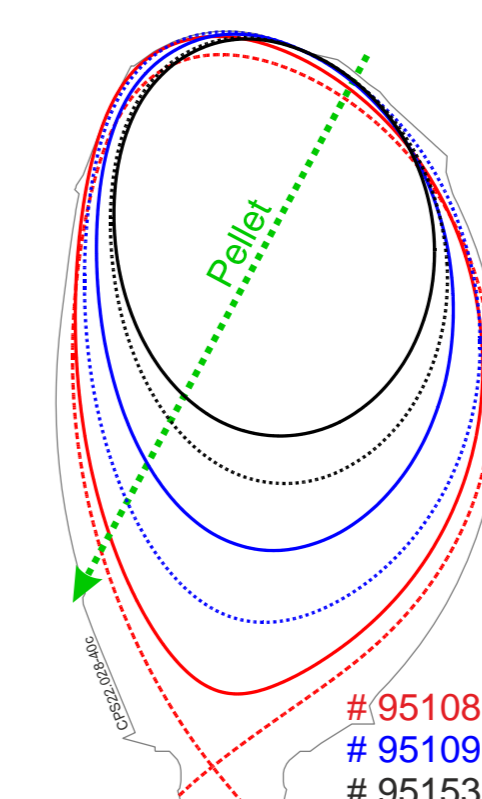


Fig.23 Plasma configurations at the time of the arrival of the pellets (dotted line) and stoppage of the vertical movement of plasma (solid line). The direction of the pellet's trajectory is shown by the green dotted line.

**The prevention of hot VDE with SPI was demonstrated. The pellet arrival stopped the vertical movement of plasma, preventing plasma from entering and melting the Be upper dump plate. In addition, the cessation of the vertical motion of the plasma also prevents the drop of the safety factor  $q_{95}$  and, as a result, the SPI prevents AVDEs, where large vessel asymmetric (radial) displacement occurs.**

For details/discussion see "Mitigation of disruption electro-magnetic load with SPI on JET-ILW" paper due to be submitted to the NF by August this year